Radiochemistry, Vol. 46, No. 4, 2004, pp. 377–384. Translated from Radiokhimiya, Vol. 46, No. 4, 2004, pp. 348–355.
Original Russian Text Copyright © 2004 by Anan'ev, Shilov.

Heterogeneous Catalytic Decomposition of Hydrazine in Nitric Acid Solutions

A. V. Anan'ev and V. P. Shilov

Institute of Physical Chemistry, Russian Academy of Sciences, Moscow, Russia

Received July 23, 2003

Abstract—The kinetics and stoichiometry of catalytic decomposition of hydrazine in 0.25–8 M HNO_3 in the presence of 1% Pt/SiO_2 were studied. The main reaction products are N_2, N_2O, and ammonium nitrate whose yield decreases with increasing $[HNO_3]$. It was found that catalytic decomposition of hydrazine in HNO_3 is a result of three different processes: heterogeneous catalytic disproportionation of hydrazine at the catalyst surface, oxidation of hydrazine with catalytically generated HNO_2, and heterogeneous catalytic oxidation of hydrazine with HNO_3. The contribution of these processes to the overall reaction is mainly governed by HNO_3 concentration and temperature. The role of platinum in the catalysis of hydrazine oxidation in nitric acid media and possible mechanisms of catalytic processes are discussed.

Thanks to its unique chemical and physical characteristics, hydrazine is one of the most important and well-studied nitrogen compounds. Hydrazine and its derivatives are widely used in space technology as propellant components or as monopropellants for satellites and spacecrafts [1]. The other important field of hydrazine application is chemistry and technology of actinides. Having a pronounced reductive power, hydrazine is used as nitrite scavenger in electrochemical reduction of U(VI) [2] or directly as a reducing agent for stabilization of actinide ions in lower oxidation states [3]. It was shown previously that the reducing activity of hydrazine with respect to actinide ions increases significantly in the presence of some heterogeneous catalysts [4–6]. The kinetics of redox reactions were studied, and attempts were made to elucidate the mechanism of heterogeneous catalytic reaction of hydrazine with actinide ions in solutions [6–9]. However, some experimental results, such as contradictory reaction orders with respect to hydrazine concentration, the influence of acidity on the process rates, and superstoichiometric consumption of hydrazine, were not adequately explained.

The kinetics and mechanisms of catalytic decomposition of hydrazine were thoroughly studied in the presence of a great number of catalytic materials. The results of these studies were summarized in a monograph [10]. The above studies are related to the catalytic decomposition of anhydrous N_2H_4 or hydrate $N_2H_4 \cdot H_2O$ in gaseous or liquid state. The results obtained cannot adequately explain the behavior of hydrazine in the presence of heterogeneous catalysts in acidic solutions, in which it exists in the form of hydrazinium ion $N_2H_5^+$. The kinetics and mechanism of catalytic decomposition of hydrazine in perchloric and sulfuric acid solutions in the presence of the catalyst Pt/SiO_2 were thoroughly studied previously [11]. It was found that, in acidic solutions containing no nitrate ions, the catalytic decomposition of hydrazine proceeds according to the stoichiometric equation

$$3N_2H_5^+ + H^+ = 4NH_4^+ + N_2. \qquad (1)$$

The kinetics of hydrazine decomposition in nitric acid solutions on the Pt/SiO_2 catalyst was studied in [12]. A complicated dependence of the reaction rate on the HNO_3 concentration was found; however, no assumptions on the reaction stoichiometry and mechanism were made. At the same time, there is no doubt that these data are of scientific and practical interest.

Here we studied the features of heterogeneous catalytic decomposition of hydrazine in nitric acid solutions.

EXPERIMENTAL

In the experiments we used $N_2H_4 \cdot HNO_3$ and HNO_3 of pure and chemically pure grade, respectively.

The catalyst 1% Pt/SiO_2 with the grain size of 0.5–1.0 mm was prepared by the standard procedures by treatment with a hydrazine hydrate solution of silica gel grains impregnated with H_2PtCl_6 [11]. The actual content of platinum on silica gel, determined by the atomic emission method (Perkin–Elmer Optima 3000 RL) after dissolution of Pt from a weighed portion of the catalyst in aqua regia, was 1.04%. The

1066-3622/04/4604-0377

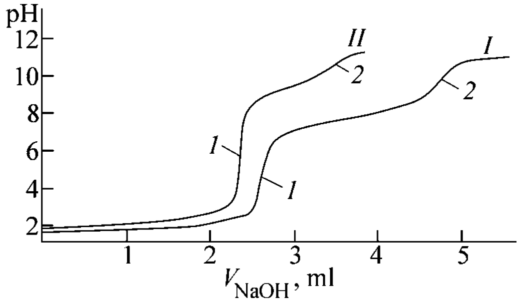

Fig. 1. Curves of potentiometric titration of the reaction mixture (*I*) before and (*II*) after catalytic decomposition of hydrazine in the presence of 0.1 g ml^{-1} of 1% Pt/SiO$_2$ at 60°C. Composition of the initial solution: 0.43 M $N_2H_5^+$; 0.53 M HNO_3. Aliquot 5 ml. Titrant 1 M NaOH. Curve *I*: initial pH 1.57, equipotential points: (*1*) pH 4.60, 2.629 ml; (*2*) pH 9.69, 4.770 ml; curve *II*: initial pH 1.81, equipotential points: (*1*) pH 5.66, 2.376 ml; (*2*) pH 10.49, 3.489 ml.

specific surface area and pore volume (mesopores) of the catalyst, according to the results of measurements of nitrogen adsorption–desorption at 77 K (Coulter SA 3100), were 350 m^2 g^{-1} and 0.96 cm^3 g^{-1}, respectively.

The kinetic experiments were carried out in a temperature-controlled glass reactor equipped with a reflux condenser to prevent evaporation of working solutions. The working solutions were prepared just before experiments by mixing of the required amounts of the initial solutions of HNO_3 and N_2H_4–HNO_3 in distilled water. The total volume of the working solutions was 50 ml. Then, a weighed portion of the dry catalyst preheated to the required temperature was added into the reactor. The reaction mixture was stirred by bubbling with argon. The stirring intensity was monitored with a float-type flow meter. Aliquots of the working solution were withdrawn for analysis at regular intervals.

The current concentration of hydrazine in the solution was determined spectrophotometrically using the color reaction with DMAB (*p*-dimethylaminobenzaldehyde) [13]. The spectra were recorded on a Shimadzu-3110 spectrophotometer.

The concentrations of acid and ammonium ions in the working solutions were determined by potentiometric titration (Metrohm 682 Titroprocessor) with a standard NaOH solution.

The gases released during the reaction were analyzed in a separate series of experiments with a Bakers QMS-200 mass spectrometer in the on-line mode. Helium was used as a carrier gas. The gas flow rate was monitored with an electronic flowmeter.

The kinetic data were processed with the Table Curve 2D software (Jandel Scientific). The rate constants of the reaction were evaluated from the results of three independent kinetic runs.

RESULTS AND DISCUSSION

Reaction Stoichiometry and Products

It is well known [14] that homogeneous oxidation of hydrazine in HNO_3 solution yields NH_4^+ ions, HN_3, N_2O, and N_2.

The preliminary qualitative analysis of the solution and released gases for HN_3 [a test with $Fe(NO_3)_3$] in catalytic decomposition of 0.25 M $N_2H_4 \cdot HNO_3$ in 3 M HNO_3 at 60°C in the presence of 0.1 g ml^{-1} of 1% Pt/SiO$_2$ revealed no HN_3.

The mass-spectrometric analysis of the released gases showed that the main gaseous products of catalytic decomposition of hydrazine in 3 M HNO_3 were N_2 and N_2O. Trace amounts of NO and NO_2 were also found.

The experiments on the study of the reaction stoichiometry were performed in 0.075–9.34 M HNO_3 solutions containing fairly high (approximately 0.5 M) initial concentrations of hydrazine to provide acceptable accuracy of potentiometric titration. Ammonium and hydrazinium ions are indistinguishable in potentiometric titration because of the close location of the equivalence points in the titration curves. Therefore, ammonium ions were determined after complete decomposition of hydrazine, which was monitored spectrophotometrically using the color reaction with DMAB. The typical curves of potentiometric titration of the initial and resulting solutions are shown in Fig. 1. The stoichiometric ratios $[NH_4NO_3]_\infty/[N_2H_5 \cdot NO_3]_0$ and $([NO_3^-]_0 - [NO_3^-]_\infty)/[N_2H_5NO_3]_0$, reflecting the accumulation of ammonium and the loss in the total amount of nitrate at various initial concentrations of HNO_3, are listed in Table 1.

Table 1 shows that an increase in the HNO_3 concentration in the range 0.075–9.34 M results in a 45% decrease in the amount of ammonium ions formed and a 60% increase in the total nitrate consumption per mole of hydrazine. Variation of the stoichiometric ratios of ammonium accumulation and nitrate consumption with variation of $[HNO_3]$ suggests that the overall reaction of catalytic decomposition of hydrazine in nitrate media is the sum of two or more processes, whose contribution is governed by the HNO_3 concentration. Analysis of the concentration dependences of the stoichiometric coefficients reveals the concentration range 0.5–5 M HNO_3 in which the ratios $[NH_4NO_3]_\infty/[N_2H_5NO_3]_0$ and $([NO_3^-]_0 - [NO_3^-]_\infty)/[N_2H_5NO_3]_0$ vary insignificantly. Taking into account the results of qualitative analysis of the released gases, it can be suggested that in the above range of HNO_3 concentration the catalytic decomposition of hydrazine nitrate mainly follows the stoichiometric equation

$$36N_2H_5NO_3 + 2HNO_3 = 20NH_4NO_3 + 32N_2 + 3N_2O + 51H_2O. \quad (2)$$

Kinetics of Catalytic Decomposition of Hydrazine

The kinetics of hydrazine decomposition in nitric acid media on the catalyst 1% Pt/SiO_2 were studied under the following conditions: $[N_2H_5^+]_0 = (0.4–5.82) \times 10^{-3}$ M; $[H^+]$ = 0.25–8 M HNO_3; T = 25–60°C; S/L = 0.02–0.1 g ml^{-1}. This low initial concentration of hydrazine was chosen taking into account the results of studying the kinetics of hydrazine decomposition in other acid media. It was found [11] that an increase in $[N_2H_5^+]_0$ above 0.01 M at S/L = 0.1 g ml^{-1} results in saturation of active centers of the catalyst, causing uncertainty in determination of the reaction order with respect to hydrazine concentration.

Preliminary kinetic experiments showed that the rate of catalytic decomposition of hydrazine increases with increasing flow rate of argon in the range 50–500 ml min^{-1} (Fig. 2). This suggests that either the reaction is diffusion-controlled or one of the volatile products of hydrazine decomposition inhibits the initial process, blocking the active centers of the catalyst. Therefore, all kinetic experiments were carried out at a constant stirring intensity (W_{Ar} = 500 ml min^{-1} through the solution volume of 50 ml).

Analysis of the kinetic curves obtained at 27°C and varied HNO_3 concentration shows that the reaction order with respect to $[N_2H_5^+]$ is not constant and changes from 0 to 1 with variation of $[HNO_3]$. Therefore, to estimate tentatively variation of the rate of catalytic decomposition of hydrazine, we chose the parameter $1/\tau_{50\%}$, where $\tau_{50\%}$ is the time of 50% reaction completion. The dependence of $1/\tau_{50\%}$ on $[HNO_3]$ presented in Fig. 3 shows that the process rate depends in a complex manner on the HNO_3 concentration, passing through a minimum in the range 3.0–3.7 M HNO_3.

It is evident that the fractional reaction order is an apparent one. Actually, the catalytic decomposition of hydrazine proceeds by zero-order and first-order reactions with respect to $[N_2H_5^+]$, and the contribution of each reaction to the overall process is governed by the experimental conditions.

Table 1. Stoichiometry of catalytic decomposition of hydrazine in nitric acid solutions at 60°C in the presence of 0.1 g l^{-1} 1% Pt/SiO_2*

$[HNO_3]_0$, M	$[N_2H_5NO_3]_0$, M	$\frac{[NH_4NO_3]_\infty}{[N_2H_5NO_3]_0}$	$\frac{[NO_3^-]_0 - [NO_3^-]_\infty}{[N_2H_5NO_3]_0}$
0.075	0.51	0.65 ± 0.01	0.40 ± 0.01
0.25	0.50	0.57 ± 0.01	–
0.53	0.43	0.52 ± 0.01	0.58 ± 0.02
1.05	0.54	0.54 ± 0.01	0.55 ± 0.03
3.01	0.56	0.55 ± 0.02	0.59 ± 0.03
6.13	0.54	0.44 ± 0.01	0.65 ± 0.03
7.45	0.68	0.40 ± 0.01	0.70 ± 0.03
9.34	0.56	0.36 ± 0.03	0.97 ± 0.04

* Stoichiometric parameters were evaluated from the results of three independent runs.

Computer analysis of the kinetic data shows that the rate of catalytic decomposition of hydrazine

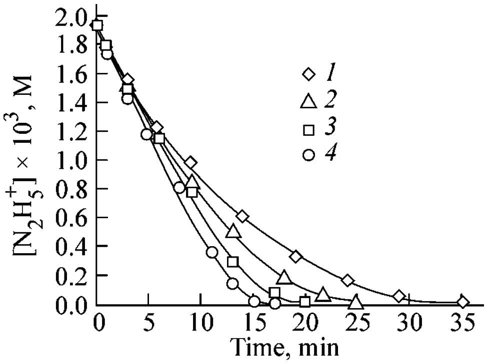

Fig. 2. Influence of the rate of argon bubbling W_{Ar} on the kinetics of decomposition of 1.94×10^{-3} M hydrazine in 3.1 M HNO_3 at 42°C in the presence of 0.06 g ml^{-1} 1% Pt/SiO_2. W_{Ar}, ml min^{-1}: (*1*) 65, (*2*) 200, (*3*) 300, and (*4*) 500.

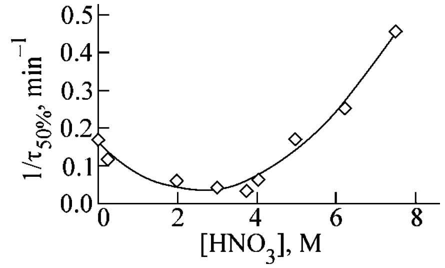

Fig. 3. Influence of HNO_3 concentration on the rate of catalytic decomposition of 1.94×10^{-3} M hydrazine at 27°C in the presence of 0.06 g ml^{-1} of 1% Pt/SiO_2.

Table 2. Influence of experimental conditions on the rate constants* of catalytic decomposition of hydrazine in nitric acid solutions in the presence of 1% Pt/SiO_2. Stirring: bubbling with argon, W_{Ar} = 500 ml min^{-1} through 50 ml of the reaction mixture

$[N_2H_5NO_3]_0 \times 10^3$, M	S/L, g ml^{-1}	$[HNO_3]$, M	T, °C	$k_0 \times 10^5$, mol l^{-1} min^{-1}	k_1, min^{-1}
5.82	0.06	1.0	42	1.20	0.093
3.88	0.06	1.0	43	1.23	0.096
0.4	0.06	1.0	42	1.18	0.090
1.94	0.02	6.2	36.5	1.9 ± 0.6	0.105 ± 0.008
1.94	0.04	6.2	36.5	2.7 ± 0.8	0.23 ± 0.01
1.94	0.06	6.2	36.5	4.1 ± 1.7	0.31 ± 0.02
1.94	0.08	6.2	36.5	5.6 ± 1.7	0.43 ± 0.03
1.94	0.1	6.2	36.5	7.8 ± 1.4	0.55 ± 0.02
1.94	0.02	3.1	42	2.92 ± 0.07	–
1.94	0.04	3.1	42	6.85 ± 0.05	–
1.94	0.06	3.1	42	11.1 ± 0.2	–
1.94	0.08	3.1	42	14.4 ± 0.2	–
1.94	0.1	3.1	42	20.1 ± 0.4	–
1.94	0.06	0.25	42	0.9 ± 0.5	0.110 ± 0.007
1.94	0.06	0.5	42	1.0 ± 0.2	0.106 ± 0.003
1.94	0.06	1.0	42	1.1 ± 0.3	0.096 ± 0.004
1.94	0.06	2.0	42	2.4 ± 0.3	0.066 ± 0.004
1.94	0.06	3.0	42	8.9 ± 0.8	–
1.94	0.06	4.0	42	13.6 ± 1.8	0.11 ± 0.03
1.94	0.06	5.0	42	8.5 ± 1.2	0.18 ± 0.01
1.94	0.06	6.0	42	4.0 ± 3.9	0.29 ± 0.05
1.94	0.06	7.0	42	–	0.477 ± 0.006
1.94	0.06	8.0	42	–	0.69 ± 0.01
1.94	0.06	0.25	30.5	0.4 ± 0.2	0.065 ± 0.003
1.94	0.06	0.25	50	0.8 ± 0.7	0.15 ± 0.01
1.94	0.06	0.25	60	1.9 ± 0.4	0.218 ± 0.006
1.94	0.06	0.25	69	0.9 ± 0.7	0.30 ± 0.01
1.94	0.06	3.1	22	0.4 ± 0.2	0.023 ± 0.003
1.94	0.06	3.1	31.5	1.1 ± 0.2	0.038 ± 0.004
1.94	0.06	3.1	41	7.7 ± 0.8	0.05 ± 0.01
1.94	0.06	3.1	52	30.6 ± 0.4	0.06 ± 0.04
1.94	0.06	6.2	28	3.3 ± 1.3	0.17 ± 0.02
1.94	0.06	6.2	36.5	4.1 ± 1.7	0.31 ± 0.02
1.94	0.06	6.2	50	4.9 ± 4.2	0.62 ± 0.06

* The values of constants presented without experimental error were obtained from a single kinetic run.

throughout the studied range of experimental conditions is adequately described by the equation

$$-dC/dt = k_1 C + k_0,$$

where k_1 and k_0 are the first-order and zero-order rate constants, respectively. The integral form of this equation is

$$\ln[(C_0 + k_0/k_1)/(C + k_0/k_1)] = k_1 t,$$

where C_0 is the initial concentration of hydrazine. This equation was used for evaluating the rate constants. In the boundary cases, when the process is the purely zero-order or first-order reaction with respect to hydrazine, the rate constants were evaluated using the corresponding equations for approximation of the kinetic curves. The results of evaluation of k_1 and k_0 for various experimental conditions are listed in Table 2.

It is seen from Table 2 that k_1 and k_0 do not noticeably depend on the initial concentration of hydrazine in the range $(0.4-6) \times 10^{-3}$ M. This allows k_1 and k_0 to be considered as true rate constants of zero-order and first-order reactions with respect to $[N_2H_5^+]$.

The trends in variation of the rate constants of zero-order and first-order reactions at 42°C with increasing [HNO_3] (Fig. 4) show that heterogeneous catalytic reactions in the system $N_2H_5^+$–HNO_3–Pt are complex. The log–log dependences of k_1 and k_0 on [HNO_3] are satisfactorily approximated by straight lines (Figs. 5 and 6), which allows estimation of the apparent reaction orders with respect to HNO_3 concentration. In the range of low concentrations of HNO_3 (0.25–2.0 M), variation of the rate constant of the first-order reaction (k_1) corresponds to negative fractional order (–0.24 ± 0.01) with respect to HNO_3 concentration. At a higher HNO_3 concentration (4.0–8.0 M), the rate constant k_1 increases, with the apparent reaction order with respect to HNO_3 concentration being 2.6 ± 0.2. The break in the plot (Fig. 5) at the point corresponding to [HNO_3] = 3.0 M is caused by the fact that under these conditions the decomposition of hydrazine is a zero-order reaction with respect to [$N_2H_5^+$]. The rate constant of the zero-order reaction (k_0) varies in accordance with the apparent orders of 1.96 ± 0.3 and –3.07 ± 0.3 in the ranges 1.0–4.0 and 4.0–7.0 M HNO_3, respectively.

It should be noted that the method used here for determining the reaction orders with respect to HNO_3 concentration is not quite rigorous in terms of formal kinetics, since under conditions of variable ionic strength of the solution we used the analytical concentration of HNO_3 rather than its thermodynamic activity. Nevertheless, this approach shows that catalytic decomposition of hydrazine in HNO_3 in the presence of Pt/SiO_2 is a superposition of three parallel independent first-order and zero-order reactions with respect to $N_2H_5^+$, whose contribution to the overall process is mainly governed by HNO_3 concentration.

The temperature dependences of the rate constants were studied at three different concentrations of HNO_3: 0.25, 3.1, and 6.2 M.

In 0.25 M HNO_3, the catalytic decomposition of hydrazine proceeds mainly by the first-order reaction with respect to [$N_2H_5^+$]. The contribution of the zero-order reaction to the overall process is insignificant, which results in low accuracy in k_0 determination (Table 2). Therefore, only k_1 values were used for evaluation of the apparent activation energy. The value of E^* = 34.2 ± 0.5 kJ mol^{-1} found in the temperature range 30.5–69°C within the accuracy of the experimental error coincides with the previously determined apparent activation energy of catalytic decomposition of hydrazine in 0.2 M HNO_3, equal to 36.4 ± 2 kJ mol^{-1} [11].

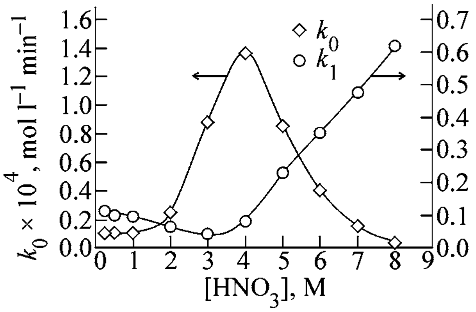

Fig. 4. Variation of the rate constants of zero-order (k_0) and first-order (k_1) reactions in catalytic decomposition of hydrazine at 42°C in the presence of 0.06 g ml^{-1} of 1% Pt/SiO_2 with increasing HNO_3 concentration.

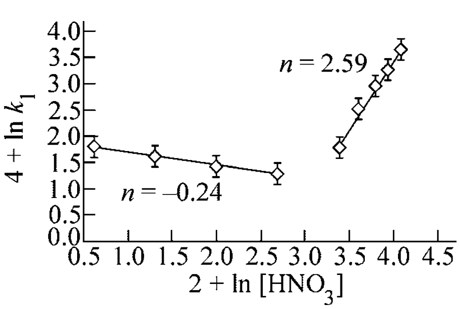

Fig. 5. Influence of HNO_3 concentration on the rate of the first-order reaction with respect to [$N_2H_5^+$] in the range 0.25–8 M HNO_3 at 42°C in the presence of 0.06 g ml^{-1} of 1% Pt/SiO_2.

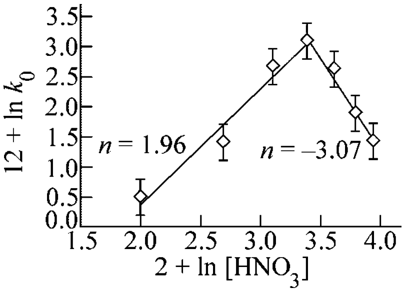

Fig. 6. Influence of HNO_3 concentration on the rate of the zero-order reaction with respect to [$N_2H_5^+$] in the range 1–8 M HNO_3 at 42°C in the presence of 0.06 g ml^{-1} of 1% Pt/SiO_2.

In 3.1 M HNO_3, the apparent activation energies determined from the temperature dependences of k_0 and k_1 are 114.6 ± 4 kJ mol^{-1} (22–52°C) and 33.7 ± 2 kJ mol^{-1} for the zero-order and first-order reactions with respect to [$N_2H_5^+$], respectively.

The apparent activation energy of the first-order reaction with respect to [$N_2H_5^+$] in 6.2 M HNO_3 was found to be 44.7 ± 3 kJ mol^{-1} in the temperature range 28–50°C. The zero-order component was not considered since its contribution to the overall process

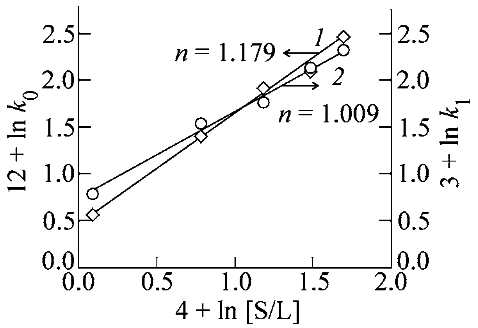

Fig. 7. Influence of the S/L ratio on the rate of catalytic decomposition of hydrazine in (*1*) 3.1 and (*2*) 6.2 M HNO_3 at 42°C.

under these conditions is extremely low and standard error in k_0 determination reaches 90% (Table 2).

It should be noted that in 3.1 M HNO_3 the contribution of the zero-order reaction with respect to $[N_2H_5^+]$ to the overall catalytic decomposition of hydrazine increases with temperature, whereas in 6.2 M HNO_3 the trend is opposite.

The determined apparent activation energy is significantly higher that the activation energy of diffusion-controlled processes (approximately 19 kJ mol^{-1} [15]). This suggests that all reactions involved in heterogeneous catalytic decomposition of hydrazine in nitric acid solutions are kinetically controlled.

The log–log dependences of the zero-order and first-order rate constants on the catalyst content in the reaction mixture (ratio S/L) are straight lines with the slopes close to 1 (Fig. 7). This suggests that the processes under consideration obey the first-order law with respect to the effective concentration of active catalytic centers.

Analysis of the results obtained allows some assumptions on the nature of chemical transformations occurring in the system $N_2H_5^+$–HNO_3–Pt.

In the range of low HNO_3 concentrations (0.25–2.0 M), the first reaction order with respect to $[N_2H_5^+]$ and negative fractional reaction order with respect to acid concentration are apparently caused by heterogeneous disproportionation of hydrazine at the platinum surface by the mechanism described for solutions of other acids [11]. This conclusion follows from the formal coincidence of the reaction orders with respect to acid concentration and the apparent activation energy for perchloric and nitric acidic media.

With increasing concentration of HNO_3 to 1 M, the contribution of the zero-order reaction with respect to $[N_2H_5^+]$ becomes significant. In 3 M HNO_3, the reaction rate practically obeys the zero-order law with respect to hydrazine concentration. It was shown previously [11] that, at low hydrazine concentrations (less than 0.01 M) in the range of S/L ratio from 0.01 to 0.1 g ml^{-1}, the catalyst surface is not saturated with adsorbed hydrazine species. Therefore, appearance of the zero-order component with respect to $[N_2H_5^+]$ is not a manifestation of the adsorption nature of the process. It is most probable that the zero order with respect to hydrazine concentration is caused by its fast reaction with HNO_2 or with one of its derivatives produced at the catalyst surface in contact with HNO_3. In this case, the rate of hydrazine loss is governed by the rate of HNO_2 formation.

Accelerated formation of HNO_2 in nitric acid solutions in contact of the latter with the catalyst Pt/SiO_2 was observed previously [16, 17]. In this case, platinum appeared in the solution in the amount comparable with the concentration of the formed HNO_2 [17]. Simple calculations using the thermodynamic activity coefficients of HNO_3 at 25°C [18] and the standard potentials of Pt^{2+}/Pt (1.888 V) and PtO_2/Pt^{2+} (0.837 V) couples [19] show that, for the range of HNO_2 concentration 10^{-6}–10^{-4} M (γ_{HNO_2} is taken equal to 1), the equilibrium potential of the HNO_3/HNO_2 couple in 3 M HNO_3 varies in the range 1.14–1.08 V (vs. NHE). At the same time, taking by convention $[Pt^{2+}] = 10^{-6}$ M and $\gamma_{Pt^{2+}} = 1$, we obtain 1.011 and 1.077 V for the equilibrium couples Pt^{2+}/Pt and PtO_2/Pt^{2+} in 3 M HNO_3, respectively (vs. NHE). Formal comparison of the resulting equilibrium oxidation potentials shows that metallic platinum in nitric acid solutions is oxidized to tetravalent state (PtO_2). This process is accompanied by reduction of HNO_3 to HNO_2. Platinum dioxide forms a protective layer at the metal surface, inhibiting further oxidation of platinum. Formation of HNO_2 in the reaction system in hand is supported by trace amounts of NO and NO_2 experimentally found in gaseous reaction products removed with bubbling inert gas. Nitrogen oxide and nitrogen dioxide are genetically related to HNO_2 by the system of well-known chemical equilibria

$$3HNO_2 \rightleftarrows 2NO + HNO_3 + H_2O, \qquad (3)$$

$$HNO_2 + HNO_3 \rightleftarrows 2NO_2 + H_2O. \qquad (4)$$

The oxidative characteristics of HNO_3 are usually considered in relation to the oxidative effect of nitronium ion NO_2^+ present in HNO_3 solution in a certain equilibrium concentration [14, 20]. NO_2^+ species can arise in the fast equilibrium reaction

$$2HNO_3 \rightleftarrows H_2NO_3^+ + NO_3^- \rightleftarrows NO_2^+ + NO_3^- + H_2O. \quad (5).$$

Taking into account the aforesaid, we can assume that decomposition of hydrazine in 1–7 M HNO_3 in the presence of the catalyst Pt/PtO_2 is a result of the following reactions proceeding at the active centers of the catalyst and in the solution. It is most likely that the process begins from the step-by-step reaction of active surface platinum atoms with nitronium ions

$$Pt + NO_2^+ \rightarrow PtO + NO^{+*} \text{ (slow)}, \qquad (6)$$

$$PtO + NO_2^+ \rightarrow PtO_2 + NO^{+*} \text{ (slow)} \qquad (7)$$

(here and hereafter, the asterisk denotes species adsorbed at the catalyst surface). Adsorbed nitrinium ions are the derivatives of HNO_2 according to the equilibrium

$$NO^+ + H_2O \rightleftarrows H_2NO_2^+ \rightleftarrows HNO_2 + H^+ \qquad (8)$$

and react with hydrazine at the catalyst surface by a chain of fast reactions, which results in the zero reaction order with respect to $[N_2H_5^+]$. Among intermediates of hydrazine oxidation, the initial product is apparently diimide N_2H_2 transforming into tetrazene and isotetrazene [21], whose decomposition at the catalyst surface yields N_2 and N_2H_4 in the first case and NH_3 and HN_3 in the second case. Nitrous oxide appears in the reaction products as a result of dimerization and decomposition of HNO. On the whole, the mechanism of oxidative decomposition of hydrazine can be tentatively presented by the following system of chemical transformations:

$$NO^{+*} + N_2H_5^+ \rightarrow N_2H_2^* + HNO^* + 2H^+, \qquad (9)$$

$$2N_2H_2^* \rightarrow HN{=}N{-}NH{-}NH_2^* \rightarrow HN_3^* + NH_3^*, \qquad (10)$$

$$2N_2H_2^* \rightarrow H_2N{-}N{=}N{-}NH_2^* \rightarrow N_2^* + N_2H_4^*, \qquad (11)$$

$$2HNO^* \rightarrow H_2N_2O_2^* \rightarrow N_2O^* + H_2O, \qquad (12)$$

$$NH_3 + HNO_3 \rightarrow NH_4NO_3. \qquad (13)$$

Oxidized active centers at the catalyst surface are regenerated as a result of the reaction with hydrazine

$$PtO_2 + N_2H_4^* \rightarrow Pt + N_2 + 2H_2O \qquad (14)$$

and become accessible for the subsequent catalytic reaction event.

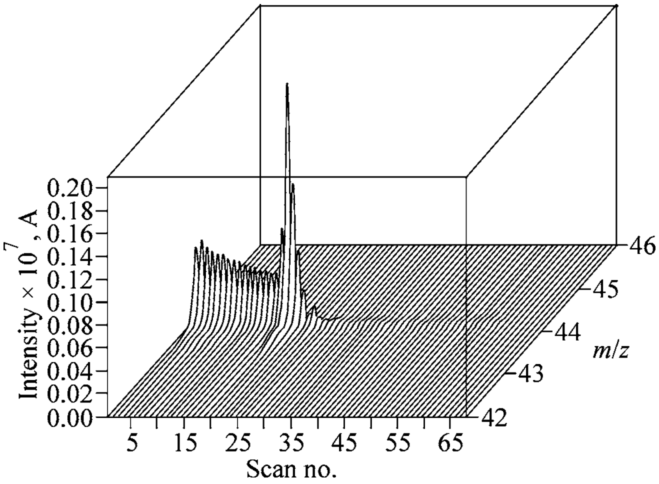

Fig. 8. Mass-spectrometric monitoring of N_2O in catalytic decomposition of 0.2 M hydrazinium nitrate in 3.0 M HNO_3 at 60°C in the presence of 0.1 g ml^{-1} of 1% Pt/SiO_2. Interval between scans 2 min.

As seen from the above scheme, one of the products of isoterazene decomposition is HN_3 [reaction (10)]. However, as was mentioned above, HN_3 was not found in the solution and released gases. Most likely, HN_3 adsorbed at the catalyst surface is not desorbed to the solution but is subjected to catalytic decomposition at the platinum surface ([22], p. 627),

$$3HN_3^* \xrightarrow{Pt} NH_3 + 4N_2, \qquad (15)$$

or is oxidized with HNO_2 at the instant of its formation. The mechanism of the latter process is unknown. However, it can be assumed that this process follows the stoichiometric equation ([22], p. 423)

$$HN_3^* + HNO_2 \rightarrow N_2 + N_2O + H_2O. \qquad (16)$$

This assumption is indirectly confirmed by the results of mass-spectrometric determination of N_2O in catalytic decomposition of hydrazine. The kinetics of N_2O formation in decomposition of 0.2 M hydrazine in 3.0 M HNO_3 at 60°C in the presence of 0.1 g ml^{-1} of 1% Pt/SiO_2 is shown in Fig. 8. As was established in separate runs, the peak in the curve of N_2O release coincides with the instant of completion of hydrazine decomposition. A similar pattern is observed in mass-spectrometric analysis of nitrogen evolution. It is evident that the adsorbed HN_3 decomposes simultaneously with hydrazine decomposition. However, taking into account that the rate of reaction of hydrazine with HNO_2 is higher than the rate of process (16) by a factor of approximately 5 [23], one would expect that, by the time of hydrazine disappearance, an excess of

HN_3 is accumulated at the catalyst surface. Its reaction with catalytically generated HNO_2 gives rise to maxima in the curves of N_2O and N_2 evolution.

An increase in the HNO_3 concentration in the range 4–8 M HNO_3 results in an increase in the rate of catalytic decomposition of hydrazine (Fig. 3). In parallel, the reaction order with respect to $N_2H_5^+$ abruptly increases from 0 to 1. Presumably, at high HNO_3 concentrations catalytic oxidation of hydrazine with HNO_3 begins to play the decisive role. In this case, the rate-determining stage of the process is the reaction of hydrazine molecules adsorbed at the catalyst surface with nitronium ions formed by equilibrium reaction (5):

$$N_2H_4^* + NO_2^+ \rightarrow NO^+ + N_2H_2 + H_2O. \qquad (17)$$

Apparently, the concentration of adsorbed hydrazine molecules is in direct proportion to the hydrazine concentration in the bulk, which is responsible for the first order with respect to $[N_2H_5^+]$. Diimide and nitrinium ions formed in the latter reaction are subjected to fast transformations (9)–(13) proceeding both at the catalyst surface and in the solution bulk.

The catalytic decomposition of hydrazine in 4–8 M HNO_3 resembles, in general features, the homogeneous oxidation of hydrazine with HNO_3 [14]. Significant distinctions are decreased activation energy of the heterogeneous reaction, characteristic of catalytic processes, and the absence of HN_3, decomposed at the platinum surface, in the final products of catalytic oxidation of hydrazine. Increased yield of ammonium ions in comparison with that in the homogeneous process is due to heterogeneous decomposition of hydrazine [reaction (1)] and HN_3 [reaction (15)] at the catalyst surface. A decrease in the yield of ammonium ions with increasing concentration of HNO_3 (Table 1) is caused by decreased contribution of these reactions to the overall process and enhancement of the role of oxidative transformations (9), (14), and (16) with increasing $[HNO_3]$.

REFERENCES

1. Urbanski, T., *Chemistry and Technology of Explosives*, New York: Pergamon, 1967, vol. 3.
2. Finlayson, M.V. and Mowat, J.A.S., *Electrochem. Technol.*, 1965, vol. 3, p. 148.
3. Koltunov, V.S., *Kinetika reaktsii aktinoidov* (Kinetics of Actinide Reactions), Moscow: Atomizdat, 1974.
4. Swanson, J.L., Platinum Catalyzed Hydrazine Reduction of Plutonium(IV) and Uranium(VI), *BNWL-1584*, 1971.
5. Nemoto, S., Ikeda, S., and Kobayashi, H., US Patent 4197274, 1980.
6. Abdounnabi, H.M., Ananiev, A.V., and Krot, N.N., *J. Radioanal. Nucl. Chem. Lett.*, 1994, vol. 186, pp. 89–97.
7. Abdounnabi, H.M. and Ananiev, A.V., *Proc. Int. Conf. on Fast Reactors and Related Fuel Cycles*, Kyoto (Japan), 1991, vol. 4, pp. 6.9–16.
8. Tananaev, I.G. and Shilov, V.P., *Radiokhimiya*, 1989, vol. 31, no. 6, pp. 52–55.
9. Anan'ev, A.V., Shilov, V.P., Afonas'eva, T.V., *et al.*, *Radiokhimiya*, 2001, vol. 43, no. 1, pp. 37–40.
10. Schmidt, E.W., *Hydrazine and Its Derivatives*, New York: Wiley, 1982.
11. Ananiev, A.V., Broudic, J.-C., and Brossard, Ph., *Appl. Catal. A: Gen.*, 2003, vol. 242, no. 1, pp. 1–10.
12. Krot, N.N., Shilov, V.P., Dzyubenko, V.I., *et al.*, *Radiokhimiya*, 1995, vol. 37, no. 1, pp. 23–27.
13. *Dosage spectrophotometrique de l'hydrazine*, *Methodes d'analyse 1968 du Commissariat a l'Energie atomique*, CETAMA, Raris: Presses Univ., Juin 1968, no. 241.
14. Koltunov, V.S., Nikol'skii, V.A., and Agureev, Yu.P., *Kinet. Katal.*, 1962, vol. 3, no. 6, pp. 877–881.
15. Moelwyn-Hughes, E.A., *The Chemical Statics and Kinetics of Solutions*, London: Academic, 1971. Translated under the title *Ravnovesiya i kinetika reaktsii v rastvorakh*, Moscow: Khimiya, 1975, p. 114.
16. Ananiev, A.V., Broudic, J.-Ch., Brossard, Ph., and Krot, N.N., *Radiochim. Acta*, 1997, vol. 78, pp. 142–145.
17. Guenais-Langlois, S., Bouyer, C., Broudic, J.-Ch., and Coq, B., *Appl. Catal. B: Environ.*, 2000, vol. 27, pp. 199–204.
18. Davis, W., Jr. and Bruin, H.J., *J. Inorg. Nucl. Chem.*, 1964, vol. 26, pp. 1069–1083.
19. Pourbaix, M., *Atlas d'equilibres electrochimiques*, Paris: Gauthier-Villars, 1963, p. 379.
20. Abel, E., *Helv. Chim. Acta*, 1950, vol. 33, p. 785.
21. Browne, A. and Kirk, J., *J. Am. Chem. Soc.*, 1928, vol. 50, p. 337.
22. Pascal, P., *Nouveaux traité de chimie minérale*, Paris: Masson, 1956, vol. 10.
23. Fitzpatrick, J., Meyer, T.A., O'Neill, M., and Williams, D.L.H., *J. Chem. Soc., Perkin Trans. 2,* 1984, pp. 927–932.